



Modelling Ross Ice Shelf melting effect on the Southern Ocean in quasi-equilibrium

Xiying Liu

Institute of Atmospheric Physics, Chinese Academy of Sciences, Beijing, 100086, China

5 *Email:* liuxy@lasg.iap.ac.cn

Abstract. To study the influence of basal melting of Ross Ice Shelf (BMR) on the Southern Ocean (ocean southward of 35° S) in quasi-equilibrium, numerical experiments with and without BMR effect have been performed with a global ocean-sea ice-ice shelf coupled model. In both experiments, the model started from a state of quasi-equilibrium ocean and was integrated for 500 years forced by CORE (Coordinated Ocean-ice Reference Experiment) normal year atmospheric fields. The simulation results of the last 100 years have been analysed. It's shown that, the melt rate averaged over the entire Ross Ice Shelf is 0.253 m/a, which is associated with a freshwater flux of 3.15 mSv (1 mSv = 10³ m³/s). The extra freshwater flux decreases the salinity in the Southern Ocean substantially whereas the effect of concurrent heat flux is not so significant except in the middle layer of water body (roughly from 1500 m to 3000 m). The decreased density due to BMR effect creates local circulation anomalies in the Ross Sea and nearby water with the help of ocean bathymetry. Through advection by the Antarctic Circumpolar Current, the flux anomaly from BMR gives rise to the increase of sea ice thickness and sea ice concentration in the Ross Sea adjacent to the coast and the ocean water westward. The warm advection and downwelling associated with the local circulation anomalies decrease the sea ice concentration in the rim of sea ice cover adjacent to open water in the Ross Sea in September. The decreased density weakens the sub-polar cell as well as the lower cell in the global residual meridional overturning circulation. And, northward meridional heat transport anomaly in most latitudes of the global ocean is accompanied accordingly.

1 Introduction

When continental glaciers (also called ice sheets) flow down to coastlines and onto the ocean surface, ice shelves are formed. Ice shelves are found in Antarctica, Greenland and Canada. Ices accumulated over the ice sheets are mostly lost to the oceans by melting underneath the ice shelves or by calving of icebergs. Floating ice shelves around Antarctica are thinning substantially, driven primarily by melting at the ice-ocean interface (Paolo et al., 2015; Rignot et al., 2013) and basal melt rates in a channel beneath the currently stable Ross Ice Shelf can be larger than 2500% of the overall background rate (Marsh et al., 2016). Ice shelf melting exceeds calving flux (Rignot et al., 2013; Depoorter et al., 2013) and contributes significantly to the fresh water balance in the shelf areas around Antarctica (Beckmann and Goosse, 2003). The circulation in sub-ice shelf cavities is markedly different from that in the open ocean, consisting largely of a thermohaline circulation forced by



melting and freezing processes at the ice shelf base. This circulation is of more than local importance, since it plays a key role in the production of Antarctic bottom water (AABW), a driver of the global thermohaline circulation (Walker and Holland, 2007). Neglecting the sub-ice freshwater input has various implications for the Southern Ocean. These are most pronounced in the Weddell and Ross Seas where large caverns are connected to broad continental shelves (Hellmer, 2004).

5 Mass exchange between the Antarctic Ice Sheet and the Southern Ocean has drawn much attention (Rowley et al., 2007; Kusahara and Hasumi, 2013).

Basal melting of the ice shelves has long been of interest because of its importance to the mass balance of the Antarctic ice sheet (Nost and Foldvik, 1994). Estimation of basal melting of ice shelf has been made by many researchers (for example, Hellmer and Jacobs (1995); Rignot et al. (2013); and others). The equivalent freshwater flux of ice shelf basal melting is

10 about 0.5 m/a over the circumpolar continental shelf area, exceeding P–E (Precipitation minus Evaporation) by a factor of at least 2 (Beckmann and Goosse, 2003). Since the injection of this fresh water occurs at the base of the ice shelf edge, it has a different impact on the stability of the coastal ocean than the P–E forcing. The quantification of basal mass loss under changing climate conditions is important for projections regarding the dynamics of Antarctic ice streams and ice shelves, and global sea level rise (Hellmer et al., 2012).

15 The need for numerical modeling of ice shelf–ocean interaction is particularly acute due to a lack of extensive observational data, which results from the physical inaccessibility of the areas of interest. Besides, available observations can provide no direct information about the sub-ice shelf circulation, leaving a significant role to be played by numerical models (Walker and Holland, 2007). In ice shelf–sea ice–ocean coupled modeling, researchers use different kinds of ice shelf representation, such as dynamic (Grosfeld and Sandhager, 2004), simplified and computationally inexpensive but capable of

20 handling significant changes to the shape of the sub-ice shelf cavity as the shelf profile evolves (Walker and Holland, 2007), fixed cavity and thermodynamics (Losch, 2008; Timmermann et al., 2012), and parameterization (Beckmann and Goosse, 2003). The models are mostly circumpolar (Hellmer, 2004; Kusahara and Hasumi, 2013), regional (Galton-Fenzi et al., 2012) or two-dimensional (Walker et al., 2009) in space. Beckmann and Goosse (2003) studied the ice shelf basal melting effect using a global ocean–sea ice coupled model with parameterized ice shelf basal melting. Timmermann et al.

25 (2012) presented results of ice shelves basal mass loss from a global sea ice–ice shelf–ocean model based on the finite element method, in which the model was forced with daily data from the NCEP/NCAR reanalysis for the period 1958–2010. In study such as modeling Ice Shelf melting effect on the Ocean in quasi-equilibrium, using global model with ice shelf thermodynamics for basal melting and performing integration over hundreds of years is of necessity. At present, this kind of research has rarely been reported.

30 The Antarctica possesses the majorities of the world’s ice shelves, of which the Ross Ice Shelf (RIS) has the largest area. Nost and Foldvik (1994) studied the circulation under the RIS with a simple analytical model. Using a two-dimensional channel flow model forced by thermohaline differences between the open boundaries and the interior cavity, Hellmer and Jacobs (1995) studied the flow under the RIS and estimated the ice shelf base lose rate to be 18–27 cm/yr. Through comparing model estimates of oceanic CFC-12 concentrations along an ice shelf edge transect to field data collected during



three cruises spanning 16 year, Reddy et al. (2010) estimated that the residence time of water in the RIS cavity is approximately 2.2 years and that basal melt rates for the ice shelf average 0.1 m/a. Arzeno et al. (2014) used data from two moorings deployed through RIS, ~6 and ~16 km south of the ice front east of Ross Island, and numerical models to show how the basal melting rate near the ice front depends on sub-ice-shelf ocean variability. These researches cannot deepen our understanding of the influences of RIS on the Southern Ocean in quasi-equilibrium since the domains of the models employed were not big enough and modeling results were impacted by boundary conditions to a great deal.

The marginal Ross Sea is an area of deep and bottom water formation. About 25% the total production rate of AABW comes from the Ross Sea and the basal melting of ice shelves modify the characteristics of water masses during the processes of AABW production along the Antarctic continental shelves (Budillon et al, 2011). Antarctic Bottom Water, is distinctly colder and fresher than North Atlantic Deep Water, and flows northward underneath it in the Atlantic below 4000m in depth. Exploring the influences of BMR on global ocean, especially on the Southern Ocean in quasi-equilibrium will be an interesting topic. In this study we aim to estimate the effect of BMR on the Southern Ocean in quasi-equilibrium by a global ice shelf-sea ice-ocean coupled model. The model represents ice shelf–ocean interaction by assuming the RIS being in a steady state, interacting with the ocean only through thermodynamics.

15 **2 Model, datasets and experiments set up**

The Massachusetts Institute of Technology general circulation model (MITgcm) (Marshall et al., 1997) is used to carry out the numerical experiments. A dataset of Antarctic cavity geometry (Timmermann et al., 2010) is used to get RIS draft. The CORE (Coordinated Ocean-ice Reference Experiment) normal year data (Large and Yeager, 2004) is used as atmospheric forcing fields.

20 The MITgcm consists of packages such as atmosphere, ocean, sea ice, ice shelf and so on for flexible configuration. The parameterizations used in this study include the Gent-McWilliams-Redi eddy parameterization (Redi, 1982; Gent and McWilliams, 1990), and the nonlocal K-profile vertical mixing parameterization (Large et al., 1994). A sea ice model package with zero-layer thermodynamics (Hibler, 1980) and viscous-plastic rheology (Zhang and Hibler, 1997) is employed. A package of ice shelf thermodynamics (Losch, 2008) named shelfice is ready for use in the MITgcm. For more information on the MITgcm see the latest online document at MIT website [http://mitgcm.org/public/r2_manual/latest/online_documents](http://mitgcm.org/public/r2_manual/latest/online_documents/manual.html) /manual.html.

Two experiments, one with and another without RIS basal melting are set up. The two experiments are denoted by EI and EN respectively. In both experiments, bathymetry of RIS cavity is included. Both experiments start from a model restart state of one integration over 1000 years (Liu and Liu, 2012). To resolve the RIS vertically better, the vertical resolution for the upper 1000 meters is improved and that below 1500 meters is coarsened with the total model layers remaining 30. Vertical interpolation is used to get the model initial fields. Since the RIS was treated as land in the former over 1000 years'



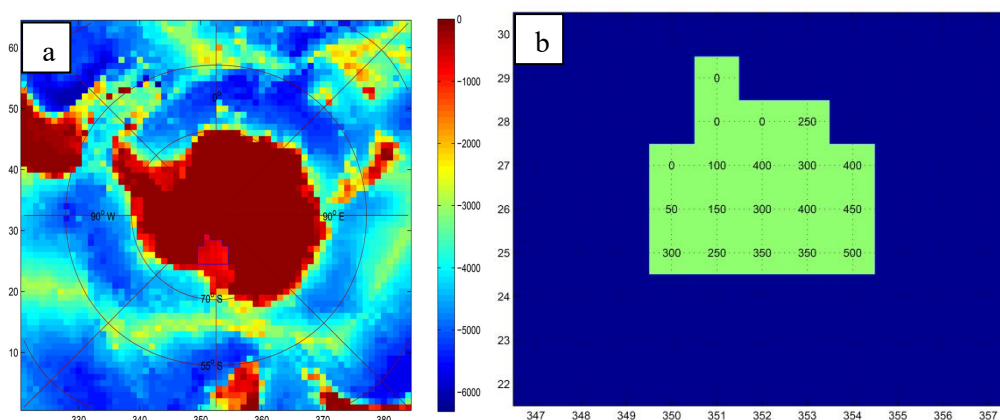
integration, the ocean initial states in the RIS cavity of the experiments here are from extrapolation. The cubed sphere grids are used and the horizontal resolution is about 150 km. Except for vertical layer division and the shelfice package, model parameters used here are identical to that in Liu and Liu (2012). The major parameters for the shelfice package used in EI are given in table 1. The model has been integrated for 500 years for each configuration.

5

Table 1. Major parameters for the shelfice package used in EI

Parameter	Value	Parameter	Value
Heat transfer coefficient that determines heat flux into ice shelf	1.0 e-04 m/s	Salinity transfer coefficient that determines salt flux into ice shelf	5.05 e-07 m/s
If a simple ISOMIP (Ice Shelf-Ocean Model Intercomparison Project) thermodynamics is used	yes	If conservative form ice-ocean interface boundary condition following Jenkins et al. (2001) is used	No
If average over boundary layer width is used	yes	If slip condition for ice shelf is used	Yes

Under the current configuration, the whole model domain in the horizontal consists of 6 cubed sphere faces and the Antarctica situates on the 6th face. The bathymetry of ocean around the Antarctica and cavity geometry of RIS is shown in Figure 1. There are 64x64 grids on each cubed sphere face and the maximum depth of the Southern Ocean is over 6000 m (Fig. 1a). There are totally 19 grid boxes covered by ice shelf, of which 15 having cavities and being calculated basal melting in the model. The depth of RIS cavity ranges from 50 m to 500 m (Fig. 1b).



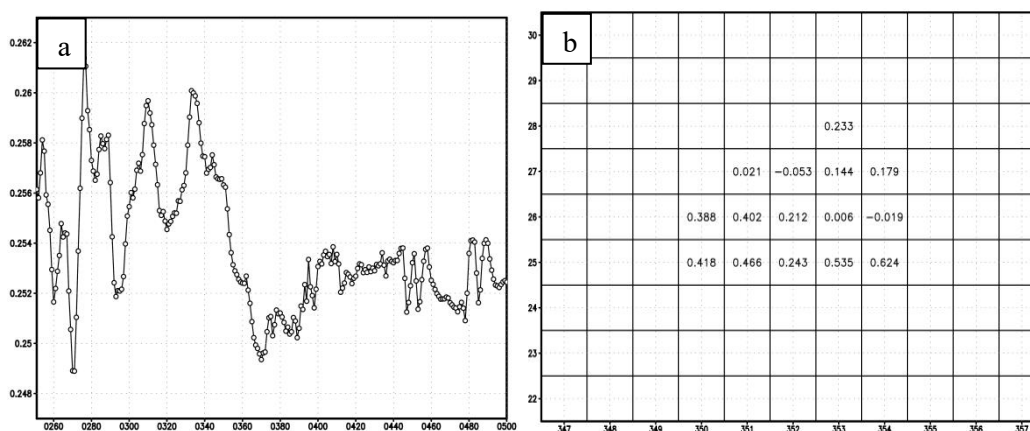
15 **Figure 1. Bathymetry of the 6th cubed sphere face in the experiments (a) and cavity geometry of RIS in EI (b). The numbers on the axes indicate positions of grids on the model domain. The yellow shades in (b) indicate grids where cavities are resolved by the model and the numbers in (b) indicate thickness of water column in the cavity. The units of bathymetry and thickness of water column in the cavity are all m.**



3 Results

3.1 Simulated basal melting of RIS and its local effects

There is significant interdecadal variability in the simulated basal melt rate and the variability is smaller in the last 100 years compared to that in other periods (Fig. 2a). The difference in the feature of interdecadal variability may be due to the influence of ocean system adjustment process. After about 400 years' adjustment, the ocean reaches a quasi-equilibrium state and the decadal variability becomes smaller. So, in later discussions, only the data of the last 100 years' integration will be used. In the simulation result, only 2 out of 15 grid boxes for RIS experience annual mean freezing while others do not and the largest melt occurs near the ice shelf front (Fig. 2b). The melt rate averaged over the entire RIS is 0.253 m/a, which is comparable to the results of Hellmer and Jacobs (1995), Assmann et al. (2003) and Arzeno et al. (2014), larger than that of Shabtaie and Bentley (1987), Holland et al. (2003), Dinniman et al. (2007,2011) and Depoorter et al. (2013), smaller than that of Rignot (2013). The largest melt occurs in April (about 0.269 m/a) and the smallest melt occurs in November (about 0.238 m/year) (Fig. 2c). This is different from that of Holland et al. (2003), in which the largest net melt rate occurs in November. The difference in seasonality may be due to combined effects of such factors as melting mechanisms in modelling ice shelf, model system evolution stage, atmospheric forcing and influence of lateral boundary.



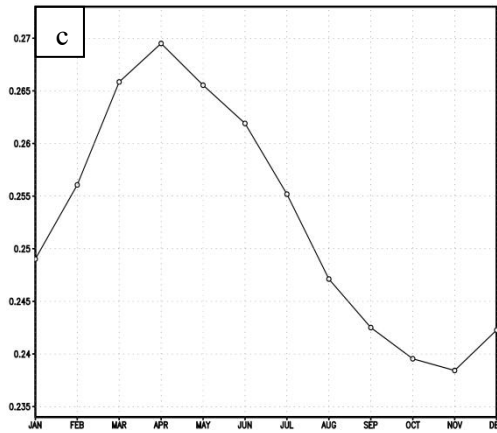


Figure 2. Basal melting rates of RIS (m/a) in EI. (a) Variation of annual mean areal average for the last 250 years. (b) Spatial distribution for the last 100 years' mean. (c) Seasonal cycle of areal mean averaged over the last 100 years.

5

Due to the inclusion of ice shelf melting in EI, cold and fresh water are supplemented into the RIS cavity and the water there become colder and fresher compared its counterpart in EN (Fig. 3). The relation of salinity bias and temperature bias of RIS cavity water from the two experiments is quasi-linear, implying larger salinity biases are corresponding to larger temperature biases. This is fundamentally governed by the latent heat formula in the model equations. The maximum decrease of water temperature and salinity in the cavity can reach up to 0.5 K and 0.25 ppt respectively due to the RIS melting effect and there seems to be no significant influence on the inflow and outflow in the cavity (Fig. 3).

10

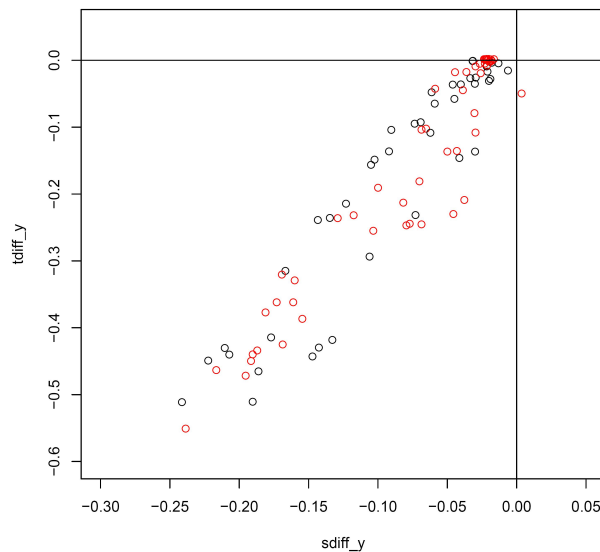




Figure 3. Figure 3. Salinity bias-temperature bias distribution of water in the RIS cavity (EI minus EN). The horizontal axis is for salinity bias and the vertical axis is for temperature bias. The inflow anomaly and outflow anomaly are marked with red and black respectively. The units for salinity and temperature are ppt and K respectively.

5 3.2 Influences of BMR on the Southern Ocean

The effect of BMR is significant on salinity for the Southern Ocean. The Southern Ocean area averaged salinity decrease in water of almost all depths except the layers from 1000m to 1250m and from ocean surface to 250m in depth (Fig. 4). The distribution of area averaged salinity difference with depth are similar in all individual oceans. Deeper than 1500m, the intensity of freshening effect of BMR grows nearly linearly with depth (Fig. 4). The response of temperature to BMR is far more complicated. At the middle layer of water body (roughly from 1500m to 3000m), the water in EI gets colder and fresher associated with the addition of cold and fresh water (Fig. 4). In the deep ocean (deeper than 3100 m), the water in EI mostly gets warmer. In the shallow ocean (shallower than roughly 550 m), the temperature biases are more varied (see figures Fig. 4a-4c). The result that the influence of freshwater flux is more significant than that of heat flux is consistent with that from Hellmer (2004), in which the anomaly of temperature is more scattered than that of salinity for water column thickness less than 1000 m in the Ross Sea. Due to that the mechanisms working on ocean temperature variation are more complex, the effects of heat flux anomaly on ocean temperature are diluted more quickly. At 1005 m, the water mostly gets saltier and warmer in the Southern Pacific Ocean and the Southern Indian Ocean (see figures Fig. 4a & Fig. 4b). This is due to that the relatively stronger Antarctic Circumpolar Current in EI at that level constrains the spread of fresh and cold water from BMR much more there (Figure not shown). At the sea bottom, water in most area southward of 45°S gets fresher (Fig. 5), which is consistent with the results from Fig. 4; large differences mostly appear in the cavity of RIS (Fig. 5).

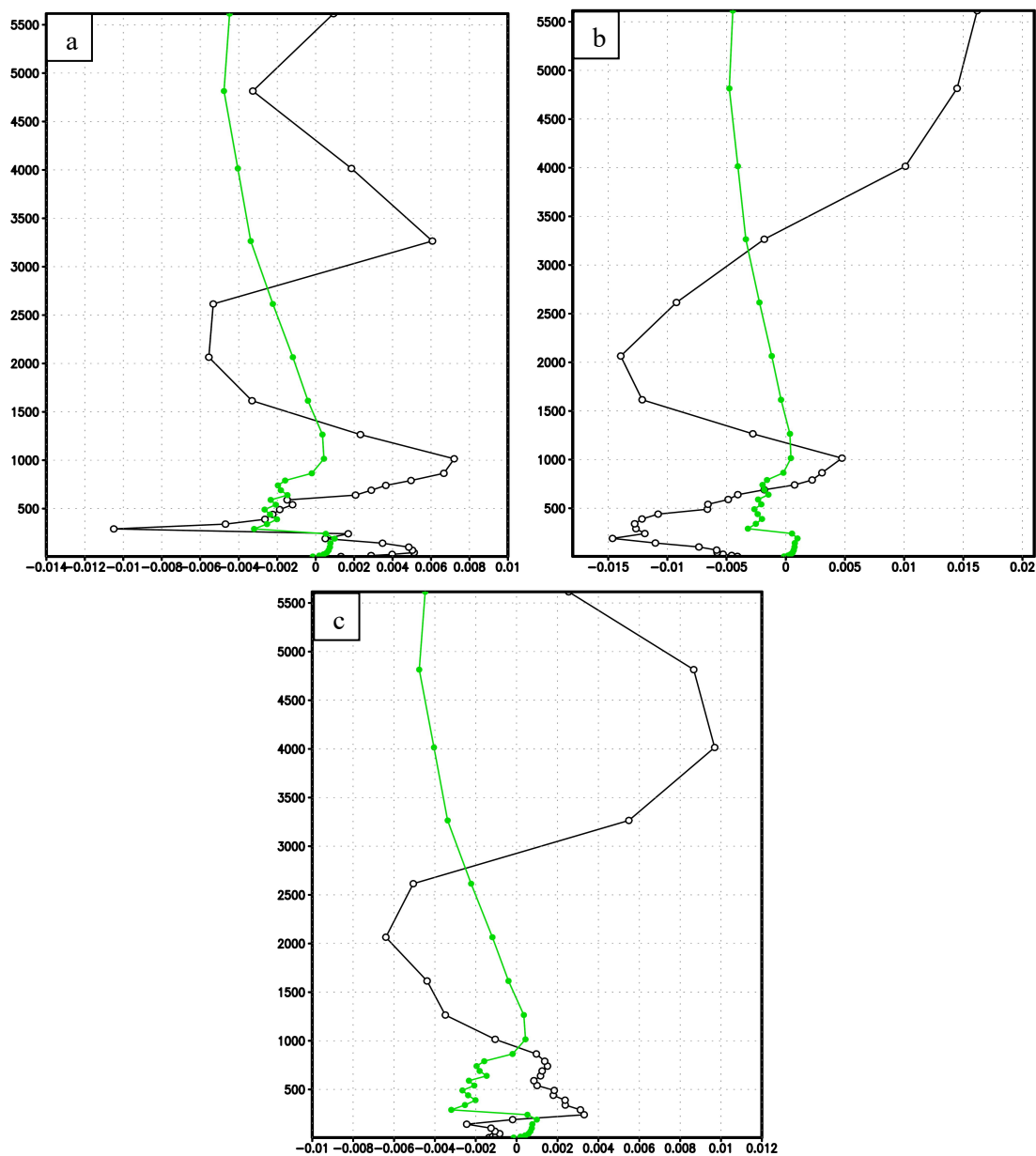


Figure 4. Area-average differences of salinity (solid circle) and temperature (open circle) (EI minus EN). The horizontal axis is for difference and the vertical axis is for ocean depth. (a) Southern Pacific Ocean. (b) Southern Atlantic Ocean. (c) Southern Indian Ocean. The units for salinity and temperature are ppt and K respectively.

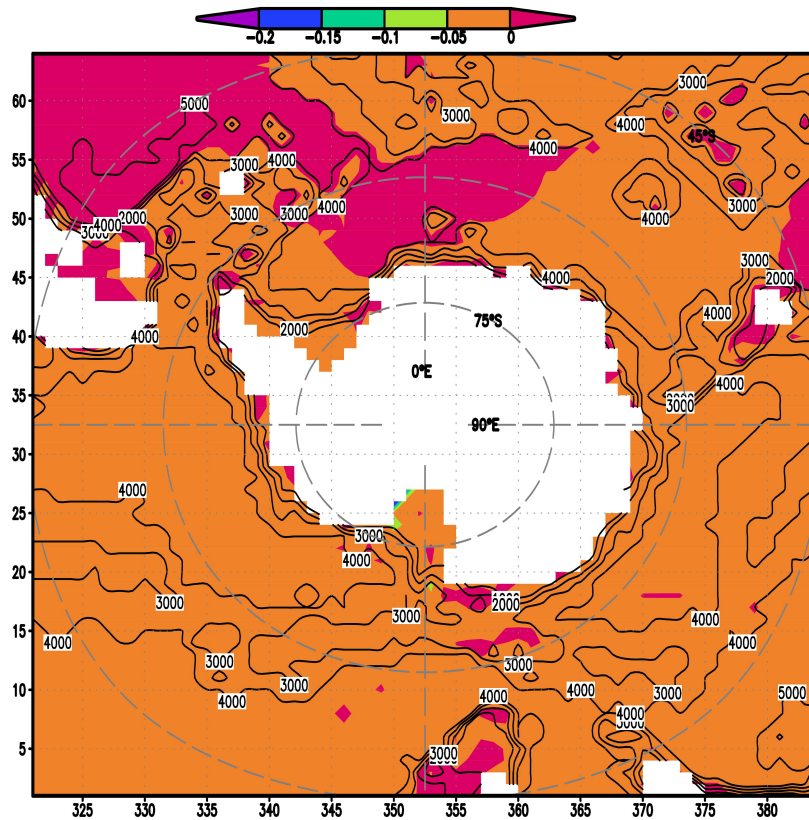


Figure 5. Annual mean salinity differences (EI minus EN, shaded) at the sea bottom. The contour lines are the thickness of water with interval 1000 m. The unit for salinity is ppt.

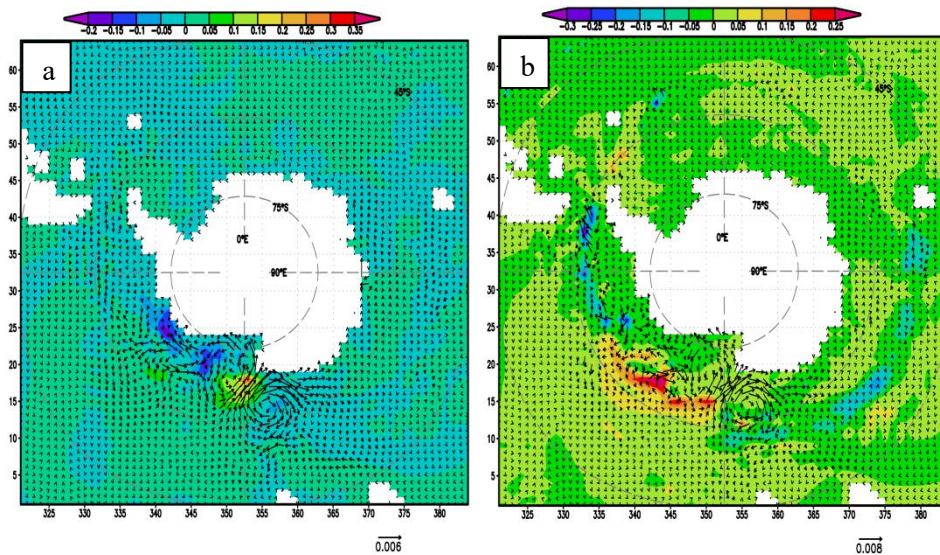
5 With BMR considered, a freshwater flux of 3.15 mSv ($1 \text{ mSv} = 10^3 \text{ m}^3/\text{s}$) is added into the surface ocean. This surplus of fresh water decreases the ocean water density and gives rise to anticlockwise circulation anomaly in the Ross Sea. In addition, associated with the specific bathymetry feature near the location ($65^\circ\text{S}, 170^\circ\text{E}$), a clockwise circulation anomaly is induced and superimposed on the Antarctic circumpolar current (ACC) in EI (Fig. 6). The two circulation anomalies work together to produce warm advection anomaly near the location ($67^\circ\text{S}, 180^\circ\text{E}$). Associated with this warm advection anomaly, warm sea surface temperature (SST) anomaly occurs there (Fig. 6a). The cold water from BMR is advected by ACC westward, giving contribution to cold SST anomaly and anomalous sea ice concentration (SIC) surplus and sea ice thickness (SIT) surplus in broad area (Fig. 6 and Fig. 7). In austral winter, sea ice extent extends due to decreased SST. The anticlockwise circulation anomaly associated with the low water density anomaly in the Ross Sea and the circulation anomaly in the north forms convergence anomaly at the ice cover edge roughly along the latitude circle 62°S . This gives rise to anomalies of surface water downwelling and increasing of SST in EI (Fig. 6b). SIC and SIT decrease there accordingly (Fig. 7b). The feature of SIT difference in the Ross Sea in the work is quite different from that of Hellmer (2004), in which one annual mean of transient phase from a regional coupled ice-ocean model is given and RIS cavity geometry is not

10

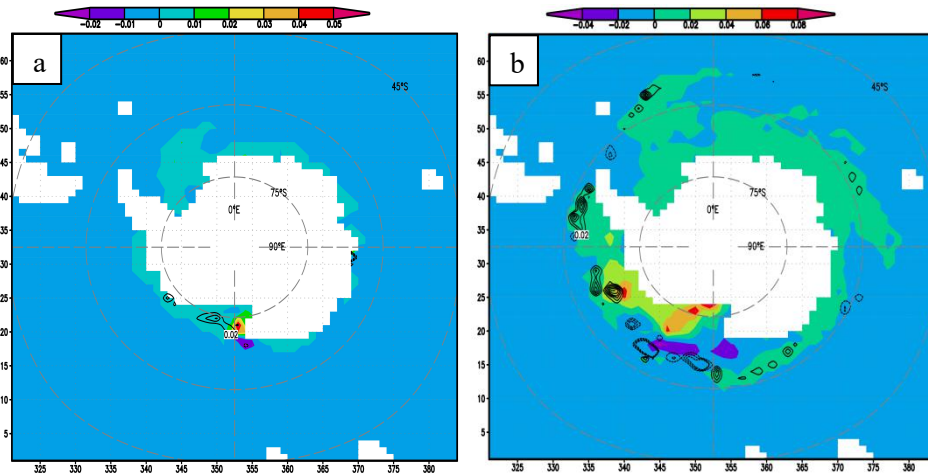
15



included in the model bathymetry for the no sub-ice freshwater input experiment. In the work, the difference of quasi-equilibrium states is discussed and the magnitude of SIT difference is far smaller than that of Hellmer (2004).



5 **Figure 6. Differences of sea surface temperature (shaded contours) and current (arrows) (EI minus EN). (a) March. (b) September. The units for temperature and current are K and m/s respectively.**

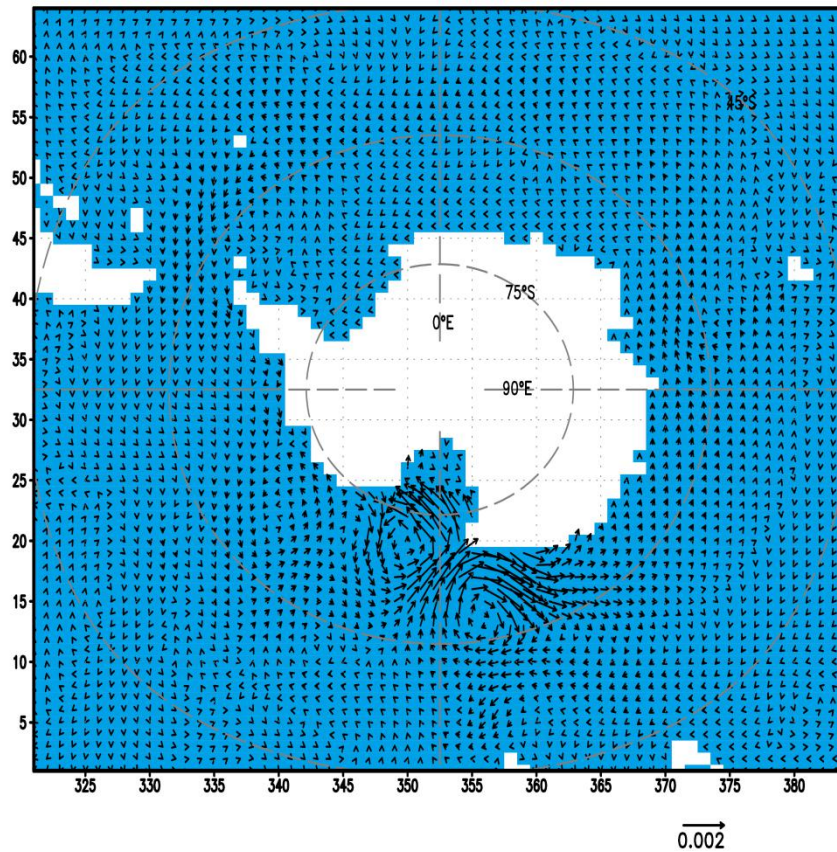


10 **Figure 7. Differences of sea ice concentration (SIC) and sea ice thickness (SIT) (EI minus EN). (a) March. (b) September. The differences of SIT are shaded. The contours in black are for differences of SIC, in which contour intervals are 0.02 and 0.05 for (a) and (b) respectively with lines of 0 not plotted. The units for SIC and SIT are 100% and m respectively.**

Similar to the pattern of surface currents (Fig. 6), the ACC is weakened when BMR effect is considered from the depth averaged ocean currents in regions other than the part north of Ross Sea (Fig. 8). There are two distinguished circulation



anomalies near the Ross Sea. One is anticlockwise and another is clockwise (Fig. 8). The pattern of the circulation anomalies holds well till about 2000 m in depth (Figures not shown), implying the combined influences of salinity anomaly from BMR and the characteristics of local bathymetry. Since the density field is dynamically linked with the motion field, the ultimate pattern of ACC anomaly is the result of the mutual adjustment between the velocity and density fields.



5

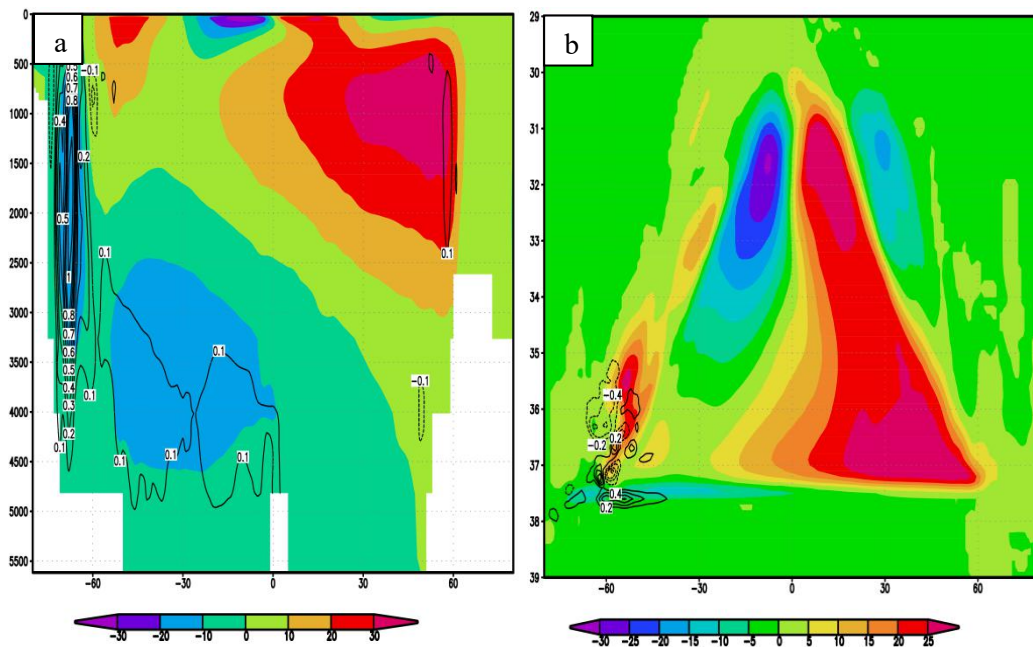
Figure 8. Differences of annual mean depth averaged ocean currents (EI minus EN). The unit of velocity is m/s.

The meridional overturning circulation (MOC), which is a system of surface and deep currents encompassing all ocean basins, is usually depicted by meridional transport stream function. When the BMR effect is introduced, the strength of Antarctic sub-polar cell and lower cell weakens (Fig. 9a) (Here, the cell names follow the convention of Farneti et al. (2015)). This is because that the enrichment of fresh water from BMR decreases the water density and damps the sink of surface dense water, and thus weakens the strength of the downward branch of MOC over the Antarctic continental slope significantly. As a consequence, the formation and spreading of the AABW will also be influenced.

Since the meridional transport stream function in depth-latitude space cannot reflect the real diapycnal transportation in the ocean (The path of overturning circulation may parallel the contour of potential density at places), it's recommended that it be evaluated in density-latitude space. When the zonal integration is performed along potential isopycnals, positions and

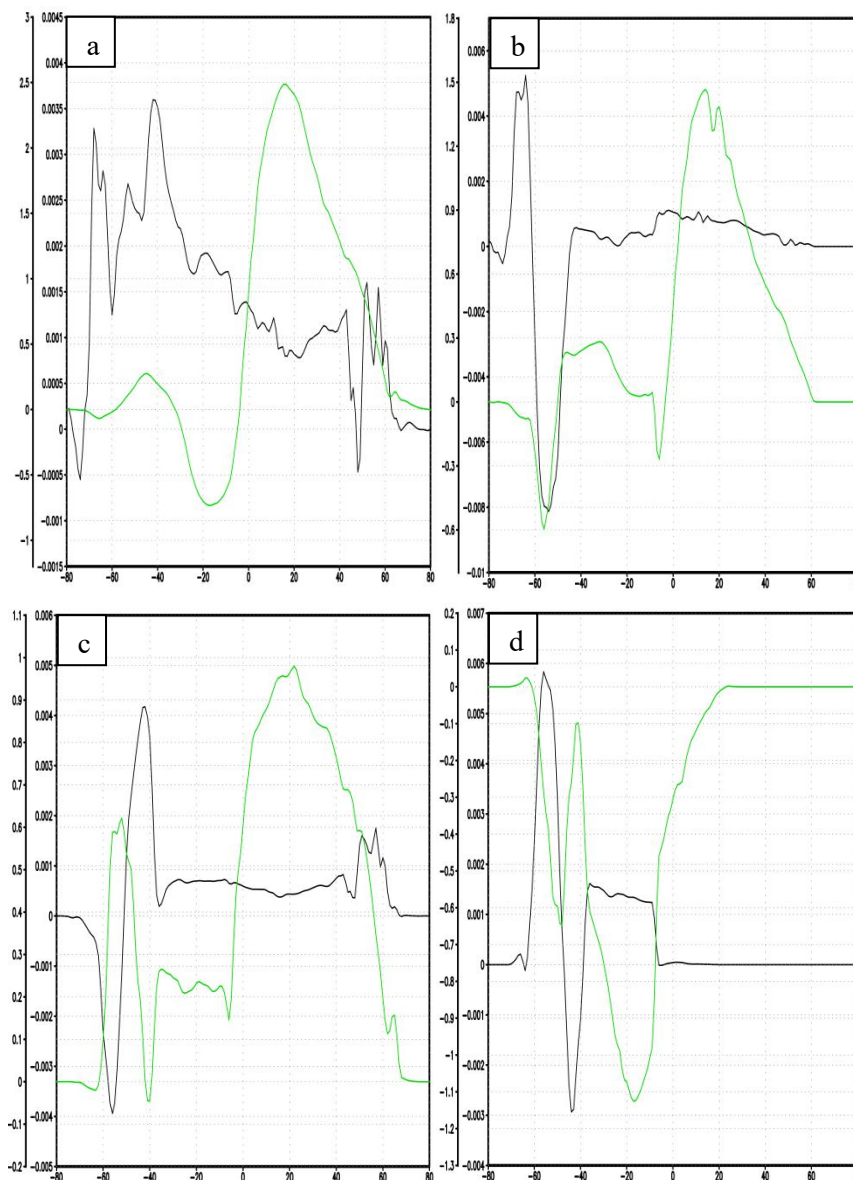


strength of cells in the meridional-isopycnal frame cannot always be traced back to their counterparts in depth-latitude space. As seen in Fig. 9b (The calculation of potential density follows the algorithm of Jackett et al. (2006) and the reference pressure used here is 2000 dbar), there are more isolated cells which have no counterparts in Fig. 9a. The upper cell breaks into two separate parts. This is quite different from most model results given in Farneti et al. (2015), in which most simulated
 5 Deacon cells (Döös and Webb, 1994) are stronger. The difference in upper cell, which deserves further investigation, may be due to the differences in model physical parameterizations and atmospheric forcing. In density-latitude space, the sub-polar cell and lower cell in the southern ocean also weakens (Fig. 9b). This is also shown in Fig. 9a.



10 **Figure 9. Meridional transport stream function from EI (shaded contours) and its difference from EN (EI-EN, contours). (a) in depth-latitude space. (b) in density-latitude space. The contour intervals for meridional transport stream function difference in (a) and (b) are 0.1 Sv and 0.2 Sv respectively with the line 0 Sv not plotted.**

The BMR contributes to ocean heat transport anomaly by changing MOC. Taking the whole world ocean as a body, the BMR contributes to northward heat transport anomaly in most part of the ocean and the maximum anomaly occurs at
 15 roughly 40°S (Fig. 10a). But for separate oceans, the features of zonal integrated heat transport anomaly might be different from one another. The southward heat transport is enhanced from 60°S to 45°S in the Pacific Ocean and reduced in the Indian Ocean (Fig. 10b and Fig. 10d). The northward transport is weakened from 60°S to 50°S and strengthened from 50°S to 40°S in the Atlantic Ocean (Fig. 10c).



5 **Figure 10. Meridional heat transport stream function from EI (green line with the left vertical axis) and its deviation from EN (EI minus EN, black line with the right vertical axis): (a) for the global ocean; (b) for the Pacific Ocean; (c) for the Atlantic Ocean; (d) for the Indian Ocean. The unit for vertical axis is PW and the unit for horizontal axis is degree.**

4 Conclusion and discussion

We have studied the influences of BMR on the Antarctic Ocean in quasi-equilibrium. The release of extra freshwater flux from BMR is 3.15 mSv (1 mSv=10³m³/s), which is associated with a basal melt rate of 0.253 m/a. The freshwater decreases the salinity in the Antarctic Ocean profoundly whereas the variation of temperature due to latent heat flux anomaly



associated with ice shelf melt is complicated implying that the mechanisms dominating the evolution of ocean temperature are more complex.

The decreased density from BMR with help of bathymetry gives rise to local circulation anomalies in the Ross Sea and the adjacent region eastward. The circulation anomalies contribute to the increased SST and decreased sea ice concentration in the ocean area affected. The cold anomaly from BMR is advected westward by ACC and increases sea ice thickness and sea ice concentration in the region affected. In the quasi-equilibrium, the strength of ACC in most areas except the northern part of the Ross Sea is reduced. The density anomaly from BMR stabilizes the water near the Antarctica and weakens the sub-polar cell as well as the lower cell in the global MOC, which is accompanied with northward meridional heat transport anomaly except for a very small part of ocean adjacent to the Antarctica.

In this study, it is assumed that the area of RIS is fixed. It seems reasonable from observation. But the total area of ice-shelf at Antarctica's periphery are reducing. The reduction of the present ice shelf area in combination with reduced basal melting changes the shelf water characteristics and decreases the stability of the water column, enhancing deep convection and the formation of denser bottom water (Hellmer, 2004).

According to simulation study by Beckmann and Goosse (2003), in which Ice shelf basal melting was parameterized as a function of the oceanic temperature on the shelf/slope area of the adjacent ocean as well as an effective area of interaction, the basal melt rate of RIS differ substantially with different atmospheric forcing fields. Thus simulations with other atmospheric forcing fields may be useful to ascertain the effects of BMR on the Antarctic Ocean. Besides, the effects of other ice shelves, such as the Filcher-Ronne and so on, should also be evaluated.

Acknowledgments. This work is partly sponsored by the China Special Fund for Research in the Public Interest (Grant No. GYHY201506011) and the Natural Science Foundation of China (Grant No. 41276190). The experiments in the work were designed and performed during visiting Professor Bitz in University of Washington at Seattle.

References

Arzeno, I. B., Beardsley, R. C., Limeburner, R., Owens, B., Padman, L., Springer, S. R., Stewart, C. L., and Williams, M. J. M.: Ocean variability contributing to basal melt rate near the ice front of Ross Ice Shelf, Antarctica, *J. Geophys. Res. Oceans*, 119, 4214–4233, doi:10.1002/2014JC009792, 2014.

Assmann, K., Hellmer, H., and Beckmann, A.: Seasonal variation in circulation and water mass distribution on the Ross Sea continental shelf, *Antarctic Science*, 15, 3–11, doi: 10.1017/S0954102003001007, 2003.

Beckmann, A., and Goosse, H.: A parameterization of ice shelf- ocean interaction for climate models, *Ocean Modell.*, 5, 157–170, doi:10.1016/S1463-5003(02)00019-7, 2003.

Budillon, G., Castagno, P., Aliani, S., Spezie G., and Padman L.: Thermohaline variability and Antarctic bottom water formation at the Ross Sea shelf break, *Deep Sea Res.*, 58, 1002–1018, doi:10.1016/j.dsr.2011.07.002, 2011.



- Depoorter, M. A., Bamber, J. L., Griggs, J. A., Lenaerts, J. T. M., Ligtenberg, S. R. M., van den Broeke, M. R., and Moholdt, G.: Calving fluxes and basal melt rates of Antarctic ice shelves, *Nature*, 502, 89–92, doi: 10.1038/nature12567, 2013.
- Dinniman, M. S., Klinck, J. M., and Smith, Jr. W. O.: Influence of sea ice cover and icebergs on circulation and water mass formation in a numerical circulation model of the Ross Sea, Antarctica, *J. Geophys. Res.*, 112, C11,013, doi:10.1029/2006JC004036, 2007.
- Dinniman, M. S., Klinck, J. M., and Smith, Jr. W. O.: A model study of circumpolar deep water on the West Antarctic Peninsula and Ross Sea continental shelves, *Deep-Sea Res. Pt. II*, 58, 1508–1523, doi:10.1016/j.dsr2.2010.11.013, 2011.
- Döös, K. and Webb, D.: The Deacon Cell and the other meridional cells of the Southern Ocean, *Journal of Physical Oceanography*, 24, 429–442, doi: 10.1175/1520-0485(1994)024<0429:TDCATO>2.0.CO;2, 1994.
- 5 Farneti, R., Downes, S.M., Griffies, S.M., Marsland, S.J., Behrens, E., Bentsen, M., Bi D., Biastoch, A., Böning, C., Bozec, A., Canuto, V.M., Chassignet, E., Danabasoglu, G., Danilov, S., Diansky, N., Drange, H., Fogli, P.G., Gusev, A., Hallberg, R. W., Howard, A., Ilicak, M., Jung, T., Kelley, M., Large, W.G., Leboissetier, A., Long, M., Lu, J., Masina, S., Mishra, A., Navarra, A., George Nurser, A.J., Patara, L., Samuels, B.L., Sidorenko, D., Tsujino, H., Uotila, P., Wang, Q., and Yeager, S.G.: An assessment of Antarctic Circumpolar Current and Southern Ocean Meridional Overturning Circulation during 10 1958–2007 in a suite of interannual CORE-II simulations. *Ocean Model.*, 93, 84–120, doi:10.1016/j.ocemod.2015.07.009, 2015.
- Galton-Fenzi, B. K., Hunter, J. R., Coleman, R.S., Marsland, J., and Warner, R. C.: Modeling the basal melting and marine ice accretion of the Amery Ice Shelf, *J. Geophys. Res.*, 117, C09031, doi:10.1029/2012JC008214, 2012.
- Gent, P. R., and McWilliams, J. C.: Isopycnal mixing in ocean circulation models, *J. Phys. Oceanogr.*, 20, 150–155, doi: 20 10.1175/1520–0485(1990)020<0150:IMIOCM>2.0.CO;2, 1990.
- Grosfeld, K. and Sandhäger, H.: The evolution of a coupled ice shelf-ocean system under different climate states , *Global and planetary change*, 42, 107–132, doi: 10.1016/j.gloplacha.2003.11.004, 2004.
- Hellmer, H. H., and Jacobs, S. S.: Seasonal circulation under the eastern Ross Ice Shelf, Antarctica. *J. Geophys. Res.*, 100, 10873–10885, doi: 10.1029/95JC00753, 1995.
- 25 Hellmer, H. H.: Impact of Antarctic ice shelf basal melting on sea ice and deep ocean properties, *Geophys. Res. Lett.*, 31, L10307, doi:10.1029/ 2004GL019506, 2004.
- Hellmer, H. H., Kauker, F., Timmermann, R., Determann, J., and Rae, J.: Twenty-first-century warming of a large Antarctic ice-shelf cavity by a redirected coastal current, *Nature*, 485, 225–228, doi:10.1038/ nature11064, 2012.
- Hibler, III, W. D.: Modeling a variable thickness sea ice cover, *Mon. Wea. Rev.*, 1, 1943–1973, doi:10.1175/1520- 30 0493(1980)108<1943:MAVTSI>2.0.CO;2, 1980.
- Holland, D. M., Jacobs, S. S., and Jenkins, A.: Modelling the ocean circulation beneath the Ross Ice Shelf, *Antarct. Sci.*, 15, 13–23, doi:10.1017/S0954102003001019, 2003.



- Jackett, D. R., McDougall, T. J., Feistel, R., Wright, D.G., Griffies, S.M: Algorithms for density, potential temperature, Conservative Temperature, and the freezing temperature of seawater. *J. Atmos. Oceanic Technol.*, 23, 1709–1728, doi: 10.1175/JTECH1946.1, 2006.
- Jenkins, A., Hellmer, H. H., and Holland, D. M.: The role of meltwater advection in the formulation of conservative
5 boundary conditions at an ice-ocean interface, *J. Phys. Oceanogr.*, 31, 285–296, doi: 10.1175/1520-0485(2001)031<0285:TROMAI>2.0.CO;2, 2001.
- Kusahara, K., and Hasumi, H.: Modeling Antarctic ice shelf responses to future climate changes and impacts on the ocean, *J. Geophys. Res. Oceans*, 118, 2454–2475, doi:10.1002/jgrc.20166, 2013.
- Large, W., McWilliams, J., and Doney S.: Oceanic vertical mixing: A review and a model with nonlocal boundary layer
10 parameterization, *Rev. Geophys.*, 32, 363–403, doi:10.1029/94RG01872, 1994.
- Large, W., and Yeager, S.: Diurnal to decadal global forcing for ocean and sea-ice models: the data sets and flux climatologies, NCAR Technical Note: NCAR/TN- 460+STR. CGD Division of the National Center for Atmospheric Research, 2004.
- Liu, X. Y., and Liu H. L.: Investigation of influence of atmospheric variability on sea ice variation trend in recent years in
15 the Arctic with numerical sea ice-ocean coupled model, *Chinese J. Geophys.* (in Chinese), 55, 2867–2875, doi: 10.6038/j.issn.0001-5733.2012.09.006, 2012.
- Losch, M.: Modeling ice shelf cavities in a z coordinate ocean general circulation model, *J. Geophys. Res.*, 113, C08043, doi:10.1029/2007JC004368, 2008.
- Marsh, O. J., Fricker, H. A., Siegfried, M. R., Christianson K., Nicholls, K. W., Corr, H. F. J., and Catania, G.: High basal
20 melting forming a channel at the grounding line of Ross Ice Shelf, Antarctica, *Geophys. Res. Lett.*, 43,250–255, doi:10.1002/2015GL066612, 2016.
- Marshall, J., Hill, C., Perelman, L., and Adcroft, A.: Hydrostatic, quasi- hydrostatic and non-hydrostatic ocean modeling. *J. Geophys. Res.*, 102, 5733–5752, doi: 10.1029/96JC02776, 1997.
- Paolo, F. S., Fricker, H. A., and Padman, L.: Volume loss from Antarctic ice shelves is accelerating, *Science*, 348, 327–331,
25 doi:10.1126/ science.aaa0940, 2015.
- Reddy, T. E., Holland, D. M., and Arrigo, K. R.: Ross ice shelf cavity circulation, residence time, and melting: Results from a model of oceanic chlorofluorocarbons, *Continental Shelf Research*, 30, 733–742, doi: 10.1016/j.csr.2010.01.007, 2010.
- Redi, M. H.: Oceanic isopycnal mixing by coordinate rotation, *Journal of Physical Oceanography*, 12, 1154–1158, doi: 10.1175/1520-0485(1982)012<1154:OIMBCR>2.0.CO;2, 1982.
- 30 Timmermann, R., Le Brocq, A., Deen, T., Domack, E., Dutrioux, P., Galton-Fenzi, B., Hellmer, H., Humbert, A., Jansen, D., Jenkins, A., Lambrecht, A., Makinson, K., Niederjasper, F., Nitsche, F., Nøst, O. A., Smedsrud, L. H., and Smith, W. H. F.: A consistent data set of Antarctic ice sheet topography, cavity geometry, and global bathymetry, *Earth Syst. Sci. Data*, 2, 261–273, doi:10.5194/essd-2-261-2010, 2010.



- Timmermann, R., Wang, Q., and Hellmer, H. H.: Ice-shelf basal melting in a global finite-element sea-ice/ice-shelf/ocean model, *Ann. Glaciol.*, 53, 303–314, doi:10.3189/2012AoG60A156, 2012.
- Nost, O.A., and Foldvik, A.: A model of ice shelf ocean interaction with application to the Filchner Ronne and Ross Ice Shelves, *J. Geophys. Res.*, 99, 14243–14254, doi:10.1029/94JC00769, 1994.
- 5 Rignot, E., Jacobs, S., Mouginot, J., and Scheuchl B.: Ice shelf melting around Antarctica, *Science*, 341, 266–270, doi:10.1126/science.1235798, 2013.
- Rowley, R. J., Kostelnick, J. C., Braaten, D., Li, X. and Meisel, J.: Risk of rising sea level to population and land area. *Eos*, 88, 105–107, doi:10.1029/2007EO090001, 2007.
- Shabtaie, S., and Bentley, C. R.: West Antarctic ice streams draining into the Ross Ice Shelf: configuration and mass balance. *J. Geophys. Res.*, 92, 1311–1336, doi:10.1029/JB092iB02p01311, 1987.
- 10 Walker, R., and Holland, D. M.: A two-dimensional coupled model for ice shelf-ocean interaction, *Ocean Modelling*, 17, 123–139, doi: 10.1016/j.ocemod.2007.01.001, 2007.
- Walker, R. T., Dupont, T. K., Holland, D. M., Parizek, B. R., Alley, R. B.: Initial effects of oceanic warming on a coupled ocean–ice shelf–ice stream system, *Earth and Planetary Science Letters*, 287, 483–487, doi:10.1016/j.epsl.2009.08.032, 2009.
- 15 Zhang, J., and Hibler III, W. D.: On an efficient numerical method for modeling sea ice dynamics, *J. Geophys. Res.*, 102, 8691–8702, doi:10.1029/96JC03744, 1997.